

Mesoscopic decoherence in Aharonov-Bohm rings

A. E. Hansen,* A. Kristensen,† S. Pedersen,‡ C. B. Sørensen, and P. E. Lindelof

The Niels Bohr Institute, University of Copenhagen, Universitetsparken 5, DK-2100 Copenhagen, Denmark

(Received 30 March 2001; published 5 July 2001)

We study electron decoherence by measuring the temperature dependence of Aharonov-Bohm (AB) oscillations in quasi-one-dimensional rings, etched in a high-mobility GaAs/Ga_xAl_{1-x}As heterostructure. The oscillation amplitude is influenced both by phase breaking and by thermal averaging. Thermal averaging is important when the temperature approaches the energy scale on which the AB oscillations shift their phase. For the phase breaking, it is demonstrated that the damping of the oscillation amplitude is proportional to the length of the interfering paths. For temperatures T from 0.3 to 4 K we find the phase-coherence length $L_\phi \propto T^{-1}$, close to what has been reported for open quantum dots. This might indicate that the T^{-1} decoherence rate is a general property of open and ballistic mesoscopic systems.

DOI: 10.1103/PhysRevB.64.045327

PACS number(s): 73.23.-b, 73.63.Nm

The understanding of decoherence in quantum-mechanical systems gives valuable insight into the crossover from quantum to classical behavior. Quantum phenomena like weak localization, universal conductance fluctuations, and the Aharonov-Bohm effect, that are observed in mesoscopic electronic systems, make these systems well suited for studying decoherence. The loss of electron phase coherence is interesting in its own right, because it reveals information about the fundamental physics of the electron-scattering mechanisms. Moreover, from the perspective of possible phase-coherent mesoscopic electronic devices,¹ a knowledge of phase-breaking length and time scales is crucial.

At low temperatures, electron-electron scattering is usually the dominating source of phase-breaking. In disordered one-dimensional (1D) and 2D conductors, the loss of phase coherence at low temperatures has been studied intensively, both theoretically and experimentally.² In clean electron systems, the number of investigations are fewer.³⁻⁶ In two dimensions, experiments consistent with the expected⁷ electron-electron scattering time $\tau_\phi \sim (T^2 \ln T)^{-1}$ have been carried out.^{3,4} In open quantum dots (a 0D system), an unexpected T^{-1} contribution was found.^{5,6} In general, phase-breaking mechanisms in ballistic, mesoscopic systems, of dimensionality less than 2, are presently not well understood.

Aharonov-Bohm (AB) rings are obvious systems for probing phase coherence. Here the interference of two electron paths leads to conductance oscillations of period h/e (or frequency e/h) in the magnetic flux enclosed by the paths. The oscillation amplitude is a direct measure of the interference strength, and it has been used to study decoherence in disordered systems.⁸ For AB rings with a two-dimensional electron-gas (2DEG) elastic mean free path longer than the circumference of the device (see, Refs. 9–15, and references therein), systematic studies of phase breaking have been scarce.

In this paper, we report measurements of the phase coherence length L_ϕ via the temperature dependence of AB conductance oscillations in quasi-1D rings, made by shallow etching in GaAs/Ga_xAl_{1-x}As heterostructures. Two mechanisms are important for the temperature dependence of the oscillation amplitude: phase breaking and thermal averaging. At finite temperature, the measured conductance is a

weighted average over an energy interval of finite width, proportional to the temperature. We discuss how thermal averaging influences the AB oscillation amplitude through the phase changes of the oscillations. In the experiment, we detect AB oscillations due to the interference of electrons that encircle the ring up to $n=6$ times. This is observed as peaks in the Fourier spectra of the magnetoconductance at multiples ne/h of the fundamental AB frequency. Accounting for the effect of thermal averaging, we find that the damping of the amplitude due to phase breaking depends linearly on n , showing directly the relaxation nature of the decoherence. We find the phase coherence length $L_\phi \propto T^{-1}$.

The AB rings are fabricated in a two-dimensional electron gas situated 90 nm below the surface of a modulation doped GaAs/Ga_xAl_{1-x}As heterostructure. At liquid He temperatures, the unpatterned 2DEG density and mobility is $n=2.0 \times 10^{15} \text{ m}^{-2}$ and $\mu=80 \text{ m}^2/\text{Vs}$, corresponding to an elastic mean free path $l_e=6 \text{ }\mu\text{m}$. The lateral confinement is obtained by a shallow wet etch, and the device is covered by a metal gate electrode. Details on the sample fabrication were presented elsewhere.¹² The sample was cooled in a ³He cryostat, and the conductance was measured in a two-terminal configuration. We used a conventional voltage biased lock-in technique, with an excitation voltage of 31.6 μV oscillating at a frequency of 116.5 Hz.

Two samples with identical designs have been investigated in detail. Here we present measurements on one of them. The main results are reproduced in the second sample. A scanning electron microscope (SEM) image of the ring is shown in Fig. 1(a). The ring has a circumference of 3 μm , $< l_e$. The gate voltage dependence of the conductance is shown in Fig. 1(b). At $T=5.8 \text{ K}$, the conductance increases in steps of height $\sim e^2/h$, due to the conductance quantization in the narrow exit and entrance wires.¹² The steps should not be taken as a sign of the population of transverse subbands in the ring itself, where the wires defining the arms are wider.¹⁶ At $T=0.3 \text{ K}$, universal conductance fluctuations are superimposed on the steps, indicating a large degree of phase coherence in the ring at this temperature.

In Fig. 1(c) we show an example of the temperature evolution of the conductance in a perpendicular magnetic field B . The AB oscillation amplitude decreases with temperature.

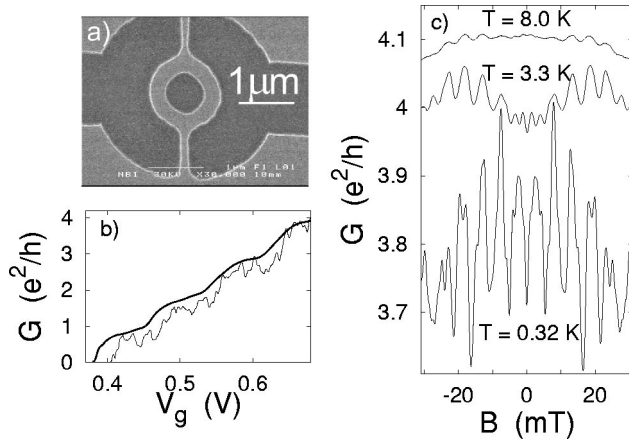


FIG. 1. (a) SEM image of the ring before gate deposition. In the dark areas the donor layer is etched away. The quantum wires defining the arms of the ring are etched 280 nm wide, while the wires connecting the ring to the 2DEG reservoirs are 100 nm wide. (b) Conductance G vs gate voltage V_g at $T=5.8$ K (thick line) and 0.32 K (thin line). (c) Examples of AB oscillations measured at a fixed gate voltage and different temperatures. Traces at high temperatures are offset for clarity.

The period of the oscillations is 5.4 mT, in agreement with the period $h/(e\pi r^2)=5.5$ mT calculated from the average radius $r=490$ nm of the ring.

To quantify the degree of coherence in the ring from the AB oscillations, we compute the fast Fourier transform (FFT) of the conductance $G(B)$, measured in the magnetic-field interval, as shown in Fig. 1(c). A measure of the AB oscillation amplitude is obtained by integrating the ne/h FFT peaks in the intervals as indicated in Fig. 2(a). The amplitudes vary with the gate voltage, as exemplified for the e/h peak in Fig. 2(b). It is sensitive to the phase difference $\Delta(k_F L)$ at zero magnetic field between electron paths in either arm of the device.^{17,12} The typical phase pickup in an arm is $k_F L \sim 200$, where $L=1.5$ μm is half the circumference of the ring and k_F is the Fermi wave number $\sim 1.5 \times 10^8$ m^{-1} . A shift in the phase of the AB h/e oscillation, between the two values 0 and π that are possible in a two-terminal measurement, requires $\Delta(k_F L)$ to change by π .¹⁷ For a real device, $k_F L$ will not increase in exactly the same manner for the two arms, and hence the phase and the amplitude depend on the gate voltage, as we observe. The presence of several transverse subbands in the arms will provide an additional source of amplitude and phase variation.

The temperature dependence of the AB oscillation amplitude is shown in Fig. 2(c) for ten different gate voltages. There is some scatter of the data points, around a well-defined average. The temperature dependence of the oscillation amplitude does not depend strongly on gate voltage, in the gate voltage interval used here.

We take advantage of the weak gate voltage dependence, and perform an average of the Fourier spectra obtained at different gate voltages. In Fig. 2(a) we show Fourier spectra averaged over the ten gate voltages, for different temperatures. We also show an average Fourier spectrum computed from spectra obtained at 500 different gate voltages at T

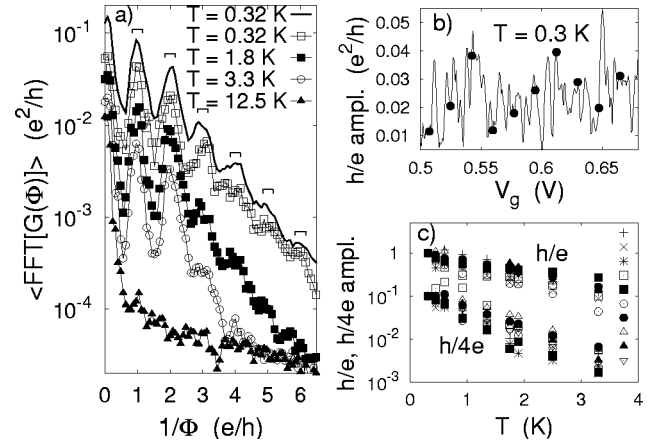


FIG. 2. (a) Fourier spectra at different temperatures, given in the legend, as functions of the inverse magnetic flux $\Phi = B\pi r^2$ through the ring. The spectra have been averaged for ten different gate voltages. The spectrum marked with a thick line results from an average of 500 gate voltages, and is offset vertically for clarity. The symbols mark the intervals in which the Fourier coefficients are integrated to calculate the oscillation strengths. (b) Amplitude of the h/e oscillations as a function of the gate voltage. The filled circles mark the ten gate voltages used in the further analysis. (c) Amplitudes of h/e and $h/4e$ oscillations for ten different gate voltages V_g , normalized to 1 and 0.1 at $T=0.3$ K, as functions of temperature. The gate voltage increases from $V_g=0.51$ V to 0.67 V in the order of the symbols plotted to the right.

$=0.32$ K. Apart from the peak at the e/h Aharonov-Bohm frequency, clear peaks appear at frequencies $2e/h$, $3e/h$, and $4e/h$, and smaller bumps are also visible at $5e/h$ and $6e/h$. Electrons can travel around the ring more than once, and a periodicity of h/ne in flux of the conductance means that the interfering electron has enclosed the ring n times. The probability for this type of event to happen will decrease with n , and so will the amplitude of the ne/h oscillation [as seen in Fig. 2(a)], with a rate that depends on the coupling between the ring and the 2DEG.

In Fig. 3(a) we show the temperature dependence of the amplitude of the h/ne , $n=1, \dots, 6$ oscillation periods, extracted from the average spectra as shown in Fig. 2(a). For high temperatures and frequencies, the FFT amplitudes collapse onto a temperature-independent background spectrum. For temperatures between 0.3 and 4 K, the amplitude drops exponentially with temperature for $n=1, \dots, 4$, but with different rates b_n for different n . We assume that the amplitude of a h/ne oscillation strength is damped due to phase-breaking in the following manner:¹⁹

$$h/ne(\text{amplitude}) \propto e^{-nL/L_\phi(T)}, \quad (1)$$

where L_ϕ is the characteristic length over which correlations in the electron phase are lost. Equation (1) implies that all h/ne amplitudes should have the same functional dependence on T , as is observed. The measured exponential dependence means that $L_\phi \sim T^{-1}$. Furthermore, the damping rates b_n [the slope of the lines in Fig. 3(a)] should increase linearly with n . This is not exactly the case, even though the rates do increase with n .

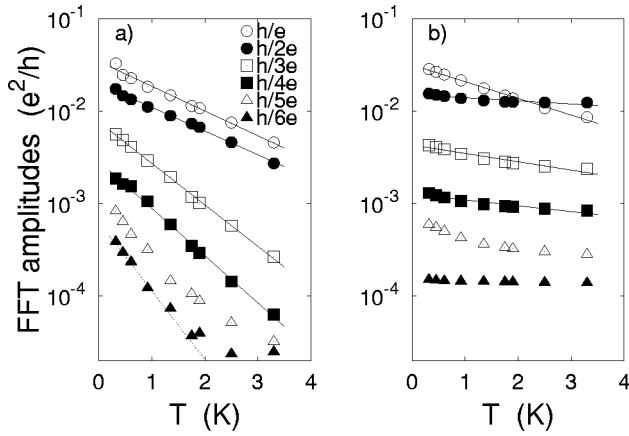


FIG. 3. (a) Measured amplitudes of the h/ne oscillations, $n = 1, \dots, 6$, on a semilog scale, as functions of temperature. Straight lines are fits with $a_n \exp(-b_n T)$, in the intervals that the lines cover. Dashed line shows the estimated decay rate of the $h/6e$ oscillation, $b_6 = 6\alpha$ (see Fig. 4). (b) As in (a), now showing amplitudes due to numerically calculated thermal averaging, as explained in the text. Straight lines are fits with $c_n \exp(-d_n T)$.

This apparent inconsistency between the data and the expected behavior due to phase breaking [Eq. (1)] can be understood when accounting for the effect of thermal averaging on the amplitude of the oscillations. At finite temperature, transport can take place in an energy window around the Fermi energy. In the Landauer-Büttiker formalism, the zero-temperature conductance G is then convoluted with the derivative of the Fermi function f :

$$G(E_F, T, B) = \int dE G(E, 0, B) \left(-\frac{\partial f(E, E_F, T)}{\partial E} \right). \quad (2)$$

Considering thermal averaging only, the amplitude of the AB oscillations will, on average, decrease with temperature only if the oscillations at low temperature change phase within the available energy window, $\sim 3.5k_B T$ wide. Phase shifts of the AB oscillations can occur if the geometrical phase difference $\Delta(k_F L)$, between the two interfering paths changes as a function of the Fermi energy, as motivated above. Therefore, the relevant temperature scale on which thermal averaging becomes efficient is given by the Fermi energy change required to shift the phase of the AB oscillations, rather than (for instance) the energy level spacing of ring eigenstates.

We use Eq. (2) to estimate the effect of thermal averaging in our experiment. For $G(E_F, 0, B)$, we use a data set $G(V_g, T=0.32 \text{ K}, B)$, where V_g is changed in steps of 0.6 mV, small enough to resolve all the changes in the AB oscillations. The relation of gate voltage V_g to the Fermi energy E_F is calibrated by following the spiky features seen on the low-temperature conductance curve in Fig. 1(b) for finite bias voltages V_{sd} . For small biases these will move linearly in the (V_g, V_{sd}) plane, with a slope $\delta V_{sd}/\delta V_g$ which is related to the Fermi energy change with gate voltage as $\delta E_F/\delta V_g = e/2(\delta V_{sd}/\delta V_g)$. The extracted $\delta E_F/\delta V_g$ is close to a simple capacitor estimate. From the simulated data sets $G(V_g, T > 0.32 \text{ K}, B)$, the average AB oscillation amplitude

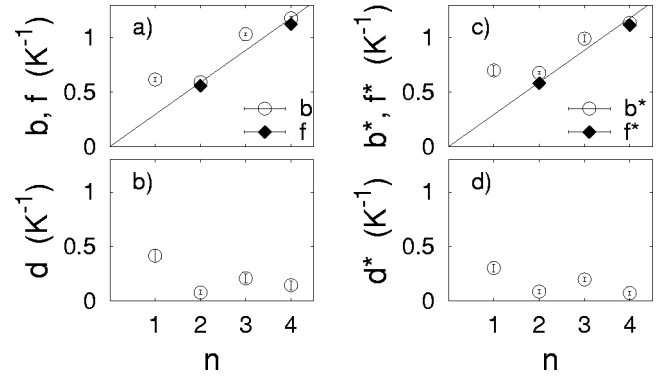


FIG. 4. (a) Circles: exponents b_n from the measured data in Fig. 3(a) vs n . Error bars on the symbols take into account the standard deviations on the fits. Straight line: fit with $b_n = \alpha n$, $\alpha = 0.3 \text{ K}^{-1}$ to the $n=2$ and 4 points. Diamonds: exponents f_n obtained from the temperature dependence of averaged AB oscillations, as described in the text. (b) Exponents d_n from the simulation in Fig. 3(b) vs n . Error bars on the symbols take into account the standard deviations on the fits and the Fermi energy calibration. (c) and (d) are as in (a) and (b), for another sample.

is extracted in the same manner as for the measured data. The result is shown in Fig. 3(b). The calculated oscillation amplitudes do decrease with temperature, but much slower than the measured amplitudes. We conclude that thermal averaging alone cannot account for the measured data. Furthermore, there is a clear tendency that the calculated h/ne amplitudes decay faster for n odd than even. For n even, the magnetoconductance oscillations result partly from interference between time-reversed paths, the same paths that ultimately give rise to Altshuler-Aronov-Spivak oscillations in disordered systems.¹⁸ The geometrical phase difference of these paths is zero, which means that the resulting part of the magneto-oscillations does not change phase. Consequently, they are insensitive to thermal averaging. This explains why the even frequencies in Fig. 3(b) have a slower temperature dependence than the odd frequencies. The temperature dependence can be approximated by exponentials [lines in Fig. 3(b)]. For diffusive systems,⁸ thermal averaging is not important for temperatures below E_c/k_B : $\sim 15\text{--}20 \text{ K}$ for our system, larger than the measurement temperatures. Here $E_c = \hbar \pi^2 D / (2L)^2$ is the standard expression for the correlation energy, and the diffusion coefficient $D = v_F^2 \tau$ in one dimension. However, numerical calculations on a ballistic ring have given an exponential temperature dependence for low temperatures.²⁰

We can now return to the experimental results in Fig. 3(a). As shown, the measured $h/e(h/3e)$ decay rate has a larger contribution from thermal averaging than the $h/2e(h/4e)$ decay rate. We see that the part of the damping that thermal averaging cannot account for approaches the scaling with n , as foreseen in Eq. (1). To demonstrate this, in Fig. 4(a) we show the measured h/ne decay rates vs n , and in Fig. 4(b) the estimated decay rates due to thermal averaging. The measured rates b_n are not directly proportional to n . But the $h/2e$ and $h/4e$ decay rates, which are only slightly influenced by thermal broadening (since $b_2/d_2, b_4/d_4 \sim 8$), do obey the scaling (straight line). Even the $h/6e$ decay rate

extrapolated from the scaling agrees with the data [dashed line in Fig. 3(a)]. From the data in Figs. 4(a) and 4(b), it seems plausible that, with a proper deconvolution of the thermal averaging from the phase breaking, the h/e and $h/3e$ decay rates will also obey the scaling. The inclusion of the ne/h frequencies, $n > 1$, as shown in Fig. 4, gives a consistency check that the temperature damping of the AB oscillations results from a phase-breaking process, in addition to the effect of thermal averaging, and this supports the assumption of Eq. (1). To our knowledge, this has not been done before. As a further cross-check of the analysis, we have also considered the amplitude of averaged, measured AB oscillations (as opposed to the average Fourier spectra used above). On performing the average, the amplitude of h/ne oscillations for odd n is strongly reduced. The temperature dependence of the amplitude of the ensemble-averaged $h/2e$ and $h/4e$ oscillations again shows an exponential decay. The exponents f_n [diamonds in Fig. 4(a)] are only slightly smaller than the ones obtained from the ensemble-averaged spectra, showing again that these oscillations are only little influenced by averaging. Finally, with the slope 0.3 K^{-1} of the line in Fig. 4(a), we deduce from Eq. (1) that $L_\phi(T=1 \text{ K}) = 5 \pm 1 \text{ } \mu\text{m}$.¹⁹ Another way of expressing our result is that the damping of the interference amplitude $\sim \exp(-ALk_B T/\hbar v_F)$, where $A \sim 0.4$. The same analysis performed on data from the second sample gives similar results [Figs. 4(c) and 4(d)]. Apart from these two rings, we have found interference amplitudes depending on temperature like $a \exp(-bT)$ in five other rings of different designs and sizes.

In summary, we have measured the temperature dependence of phase breaking in quasi-1D AB ring structures. We have detected oscillation amplitudes resulting from the interference of electron paths encircling the ring more than once. This has enabled us to verify a basic property of phase breaking: the damping of the amplitude scales with the length of the interfering paths. In the analysis we have included the effect of thermal averaging, which is determined by phase shifts of the AB oscillations, and hence by asymmetry changes of the ring. We find that the phase-breaking length is proportional to T^{-1} , close to what was measured in open quantum dots.^{5,6} Thus the T^{-1} dependence of the phase breaking might be a general characteristic of mesoscopic ballistic systems. A theoretical effort to address this question is needed.

Note added in proof: Very recently, G. Seelgr and M. Büttiker have predicted $L_\phi \propto T^{-1}$ for ballistic one-channel rings (cond-mat/0106100).

ACKNOWLEDGMENTS

The authors wish to thank H. Smith and K. Flensberg for useful discussions. This work was supported by the Danish Technical Research Council (Grant No. 9701490), the Danish Natural Science Research Council (Grant No. 9903274), and by the EU (LTR Programme Q-SWITCH, Grant No. 30960). The III-V materials used were made at the III-V Nanolab, operated jointly by the Microelectronics Center of the Danish Technical University and the Niels Bohr Institute AFG, University of Copenhagen.

*Present address: Institute of Physics, Klingelbergstrasse 82, CH-4056, Basel, Switzerland.

†Present address: Mikroelektronik Centret, Oersteds Plads, DTU, Building 345 East, DK-2800, Kgs. Lyngby, Denmark.

‡Present address: Department of Microelectronics and Nanoscience, Chalmers University of Technology, SE 412 96 Goeteborg, Sweden.

¹G. Burkard, D. Loss, and D. P. DiVincenzo, Phys. Rev. B **59**, 2070 (1999).

²See, e.g., Refs. 6, and 8.

³S. Q. Murphy, J. P. Eisenstein, L. N. Pfeiffer, and K. W. West, Phys. Rev. B **52**, 14 825 (1995).

⁴A. Yacoby, M. Heiblum, H. Shtrikman, V. Umansky, and D. Mahalu, Semicond. Sci. Technol. **9**, 907 (1994).

⁵J. P. Bird, K. Ishibashi, D. K. Ferry, Y. Ochiai, Y. Aoyagi, and T. Sugano, Phys. Rev. B **51**, 18 037 (1995); D. P. Pivin, Jr., A. Andresen, J. P. Bird, and D. K. Ferry, Phys. Rev. Lett. **82**, 4687 (1999); C. Prasad, D. K. Ferry, A. Shailos, M. Elhassan, J. P. Bird, L.-H. Lin, N. Aoki, Y. Ochiai, K. Ishibashi, and Y. Aoyagi, Phys. Rev. B **62**, 15 356 (2000).

⁶A. G. Huibers, M. Switkes, C. M. Marcus, K. Campman, and A. C. Gossard, Phys. Rev. Lett. **81**, 200 (1998); A. G. Huibers, S. R. Patel, C. M. Marcus, P. W. Brouwer, C. I. Duruöz, and J. S. Harris, Jr., *ibid.* **81**, 1917 (1998).

⁷C. Hodges, H. Smith, and J. W. Wilkins, Phys. Rev. B **4**, 302 (1971); G. F. Giuliani and J. J. Quinn, *ibid.* **26**, 4421 (1982); H. Fukuyama and E. Abrahams, *ibid.* **27**, 5976 (1983).

⁸See, e.g., S. Washburn and R. A. Webb, Rep. Prog. Phys. **55**,

1311 (1992); C. Kurdak, A. M. Chang, A. Chin, and T. Y. Chang, Phys. Rev. B **46**, 6846 (1992).

⁹C. J. B. Ford, T. J. Thornton, R. Newbury, M. Pepper, H. Ahmed, D. C. Peacock, D. A. Ritchie, J. E. F. Frost, and G. A. C. Jones, Appl. Phys. Lett. **54**, 21 (1989); C. J. B. Ford, A. B. Fowler, J. M. Hong, C. M. Knoedler, S. E. Laux, J. J. Wainer, and S. Washburn, Surf. Sci. **229**, 307 (1990).

¹⁰J. Liu, W. X. Gao, K. Ismail, K. Y. Lee, J. M. Hong, and S. Washburn, Phys. Rev. B **50**, 17 383 (1994).

¹¹G. Cernicchiaro, T. Martin, K. Hasselbach, D. Mailly, and A. Benoit, Phys. Rev. Lett. **79**, 273 (1997).

¹²S. Pedersen, A. E. Hansen, A. Kristensen, C. B. Sørensen, and P. E. Lindelof, Phys. Rev. B **61**, 5457 (2000); J. Low Temp. Phys. **118**, 457 (2000); Mater. Sci. Eng., B **74**, 234 (2000); A. E. Hansen, S. Pedersen, A. Kristensen, C. B. Sørensen, and P. E. Lindelof, Physica E **7**, 776 (2000).

¹³W. G. van der Wiel, S. De Francesci, T. Fujisawa, J. M. Elzerman, S. Tarucha, and L. P. Kouwenhoven, Science **289**, 2105 (2000).

¹⁴Yang Yi, M. Heiblum, D. Sprinzak, D. Mahalu, and Hadas Shtrikman, Science **290**, 779 (2000).

¹⁵M. Casse, Z. D. Kvon, G. M. Gusev, E. B. Olshanetskii, L. V. Litvin, A. V. Plotnikov, D. K. Maude, and J. C. Portal, Phys. Rev. B **62**, 2624 (2000).

¹⁶The energy spacing $\Delta E_{0,1}$ of the first transverse subband in the exit and entrance wires is $\sim 9 \text{ meV}$. For the arms of the ring, we estimate $\Delta E_{0,1}$ to be $1\text{--}3 \text{ meV}$.

¹⁷M. Büttiker, in *SQUID'85—Superconducting Quantum Interfer-*

ence Devices and their Applications, edited by H. D. Haklbohm and H. Lübbig (de Gruyter, Berlin, 1985), p. 529.

¹⁸B. L. Altshuler, A. G. Aronov, B. Z. Spivak, D. Yu. Sharvin, and Yu. V. Sharvin, *Pis'ma Zh. Éksp. Teor. Fiz.* **35**, 476 (1982) [*JETP Lett.* **35**, 588 (1982)].

¹⁹It can be argued that L should be a circumference rather than the length of an arm. In this case, we underestimate L_ϕ by a factor of 2.

²⁰M. Shin, K. W. Park, S. Lee, and E.-H. Lee, *Phys. Rev. B* **53**, 1014 (1996).